Semi-analytical model for stretch ratio determination in inflation test for isotropic membranes

Franck Jourdan, Jonaz Vasquez-Villegas, Rania Abdel Rahman El Anwar, Simon Le Floc'h, Christiane Wagner-Kocher

Semi-analytical model for stretch ratio determination in inflation test for isotropic membranes

Franck Jourdan [a,*], Jonaz Vasquez-VILLEGAS [a], Rania Abdel Rahman EL Anwar [b], Simon Le Floc'h [a], Christiane Wagner-Kocher [a,c]

[a] LMGC-CNRS Université de Montpellier, Montpellier, France
[b] Université Française d'Egypte, Le Caire, Egypte
[c] LPMT, UHA, Mulhouse, France

A B S T R A C T

This article wishes to contribute to the understanding of principal strains distribution in inflation test for circular isotropic soft membranes, combining analytical, numerical, and experimental investigations. The method developed gives a relatively simple and original solution of the deformation and thus of the stresses during an inflating test, provided that the measurement is sufficiently close to the pole. For this purpose, a semi-analytical model (SAM) is proposed and to evaluate that theory, two complementary approaches are used. The first approach is experimental. Inflation and uniaxial tensile tests are set up on medical silicone sheets to identify their hyperelastic constitutive parameters, using Digital Image Correlation. Then these mechanical properties are injected into a 3D finite element model (FEM) of membrane, simulating the inflation test, to compare the strains that had been obtained with those of the SAM. Numerical results show that the strain calculated by the SAM follows the pattern of the circumferential strain obtained by the FEM. Up to a certain distance from the center of the disk (half of the disk for our example), strain calculated by the SAM give a correct approximation of the deformation with respect to radial and circumferential FEM strains.

Keywords:
Numerical modeling techniques
Inflation test
Membrane deformation
FEM analysis
Strain behavior
Experiment results

1. Introduction

The literature is very well covered in articles dealing with mechanical tests of the inflation type. As explained in [1], there has been a lot of theoretical research on the distribution of deformations. At first, the work of [2] developed a numerical solution for the principal stresses and strains, using Taylor series. Then, [3,4] determined strains, and curvatures by solving, numerically, a system of first-order differential equations. [5] resumed these approaches to outline a method for determining functional forms of constitutive relations and to demonstrate the validity of this method through numerical experiments for a membrane having a known strain energy function. Before that, in 1981, [6] established deformation expressions by assuming that the radial deformation was constant for small deformations.

The objective of our work is to propose a simple method for the determination of stretch ratios for use in the experimental identification of material parameters. This study results from work on the characterization of the mechanical properties of biological membranes, as work of [5,7–10]. Often these membranes are anisotropic, but some are isotropic or weakly anisotropic. This is generally the case when they are in anatomical areas where no direction of stress is preferred. Here we will focus on the case of isotropic membranes as work of [11,12]. In the literature identification of the constitutive parameters is conducted using either the external shape of the inflated membrane [13], or the displacement at the special points [14], or increasingly now, the displacement fields obtained by DIC [1,7,8,15,16]. Our identification approach is in this trend. It considers both DIC and the shape of the membrane avoiding uncertainties about the exact position of the top of the membrane, when calculate deflections.

This article wishes to contribute to the understanding of principal strains distribution combining analytical, numerical, and experimental investigations. The first section is devoted to the semi-analytical method (SAM). Then, we develop experimental approaches allowing the identification of hyperelastic material parameters, using stretch ratios developed in the SAM. Finally, we present the numerical finite element study simulating an inflation test and compare the numerical strains

* Corresponding author.
E-mail address: franck.jourdan@umontpellier.fr (F. Jourdan).

with the semi-analytical ones.

2. Method

We consider the classical benchmark inflation test, where a uniform circular thin membrane is clamped at the rim. The strain distributions in the circumferential and radial, extensions were measured as a function of the degrees from pole, by [17], for an isotropic gum natural rubber. Moreover, due to the axial symmetry of the problem and respecting the primary assertions of the membrane theory, the stress and strain could be assumed biaxial at around the top of the inflated sample, if the stretch ratio and distance to the center are moderate. The work of [18] effectively shows that in a plane of symmetry the deformation can be considered as an ellipse, rather than a circle. For the study we will thus be within the framework of a stretch ratio less than 2 and a maximum degree from the pole of about 40°, to ensure the biaxiality of the state.

The starting point of our study is the same as in [7]. We try to define the stretch ratios in the circumferential and radial extensions. On the scheme of Fig. 1, the membrane before inflation is represented by a disk (radius r and center A) and by a spherical capsule (radius R and center O) during loading. A material point P on the initial disk, at a given distance d0 from A, is located on P' after deformation. The pole of the capsule is noted B and C is the point at the rim, such that P is on the segment [AC].

The main question is how to find the value of the distance d of point P' from the axis (OA)?

To answer this question, we have used the stretch ratios and the equibiaxiality hypothesis. The circumferential stretch ratio λc is defined, quite intuitively, by the ratio d/d0 and do not depend on the position of the point P, on the circle of radius d0 and center A. On the other hand, and this is where our developments differ from that of [7], the stretch ratio in the radial extension λr is not considered as constant over the circular arc BC. The segment [PC] becomes the arc of curve P'C, which leads us to define the radial stretch at point P by the ratio P'C/PC. Thus, if θ is the angle between (OP') and (OA) and α those between (OC) and (OA), the stretch ratios verify:

$$\lambda_c = \frac{P'C}{PC} = \frac{R\sin(\theta)}{d0} \tag{1}$$

And

$$\lambda_r = \frac{P'H}{PA} = \frac{R(\alpha-\theta)}{r-d0} \tag{2}$$

Assuming the equibiaxiality,

$$\lambda_c = \lambda_r$$

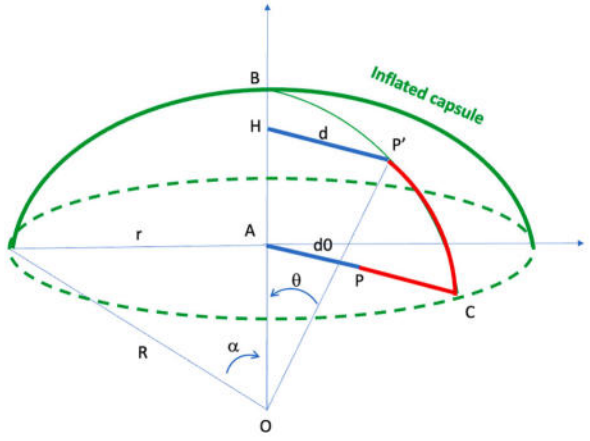

Fig. 1. 2D scheme of the inflated capsule. The lengths of the thick red lines are used to compute radial stretch ratios and those of thick blue lines that of circumferential one.(For interpretation of the references to colour in this figure legend, the reader is referred to the web version of this article.)

we obtain the following equation:

$$\frac{R\sin(\theta)}{d0} = \frac{R(\alpha-\theta)}{r-d0}$$

where the only unknown is the angle θ. Indeed, for a given radius r (depending on the applied pressure), the angle $\alpha = \sin^{-1}\left(\frac{r}{R}\right)$ and the previous nonlinear equation becomes:

$$\left(\frac{r}{d0}-1\right)\sin(\theta)+\theta = \sin^{-1}\left(\frac{r}{R}\right) \tag{3}$$

Solving this equation determines the angle θ and then the position of point P'. There is no analytical solution to this equation. We will propose to solve it numerically, which justifies the semi-analytical nature of the method.

These stretch ratios can be related to stresses using hyperelastic models. We focused on the models of Mooney Rivlin [19–22], Yeoh [23] and Neo-Hookean [24]. The value of the radial and circumferential stresses (σ_c, σ_r) can then be determined for each model as follows:

Mooney-Rivlin:

$$\sigma_c = 2C_{10}\left(\lambda_c^2 - \frac{1}{\lambda_c^2\lambda_r^2}\right) + 2C_{01}\left(\lambda_c^2\lambda_r^2 - \frac{1}{\lambda_c^2}\right)$$

$$\sigma_r = 2C_{10}\left(\lambda_r^2 - \frac{1}{\lambda_c^2\lambda_r^2}\right) + 2C_{01}\left(\lambda_c^2\lambda_r^2 - \frac{1}{\lambda_r^2}\right)$$

Yeoh:

$$\sigma_c = 2(C_{10} - 2C_{20}(I_1-3))\left(\lambda_c^2 - \frac{1}{\lambda_c^2\lambda_r^2}\right)$$

$$\sigma_r = 2(C_{10} - 2C_{20}(I_1-3))\left(\lambda_r^2 - \frac{1}{\lambda_c^2\lambda_r^2}\right)$$

Néo-Hookéen:

$$\sigma_c = 2C_{10}\left(\lambda_c^2 - \frac{1}{\lambda_c^2\lambda_r^2}\right)$$

$$\sigma_r = 2C_{10}\left(\lambda_r^2 - \frac{1}{\lambda_c^2\lambda_r^2}\right)$$

where C_{10}, C_{01}, C_{20} are material coefficients and $I_1 = \lambda_r^2 + \lambda_c^2 + \frac{1}{\lambda_c^2\lambda_r^2}$, is the first invariant of right Cauchy–Green deformation tensor. To find an equivalence between σ_c, σ_r and the pressure P, Laplace equilibrium is applied to the membrane surface.

$$\frac{\sigma_c}{\rho_c} + \frac{\sigma_r}{\rho_r} = \frac{P}{h}$$

where:

- ρ_r, ρ_c are the radii of radial and circumferential curvatures
- h is the current thickness of the membrane. Under the assumption of incompressibility, the current thickness can be calculated from the initial thickness h_{init} and stretch ratios such as:

$$h = \frac{h_{init}}{\lambda_c\lambda_r}$$

In hypothesizing an isotropic material, it is assumed that when deforming, the membrane takes the shape of a sphere; and therefore, the radii of the radial and circumferential curvatures are equal and equal to

the radius of the sphere described by the deformation. Then the relationship is

$$\frac{h_{init}}{\lambda_c \lambda_r} \frac{1}{r}(\sigma_c + \sigma_r) = P$$

This last expression will be useful during the experimental validation phase.

To evaluate the theory, we used two complementary approaches. We set up inflation tests on medical silicone sheets and reproduced these tests numerically. The objective was to verify that the stretch ratios obtained by the semi-analytical method were close to those obtained numerically. To do this, we used the definition of the stretch ratios Eqs. (1) and ((2)) to experimentally identify the material properties of the silicones being tested, then we injected these mechanical properties into a finite element model to compare the strains that had been obtained with those of the SAM.

3. Experimental approach

Studies on the experimental identification of material parameters by inflation tests are very numerous. [25], was one of the first to show the interest of these circular inflation test for the identification procedure. These experimental tests also allowed certain research groups to study the distribution of strains, such as [1], trying to show that radial strain was nearly constant over the entire surface and the circumferential strain falls to zero at the edge. While other focused on stresses, such as [26], using specific developments for the determination of membrane curvatures, coupled with finite element calculations for validation.

3.1. Material and methods

The bench test is composed of a pressurization system, an inflating device, two cameras (see Fig. 2), and a stereo-correlation image software.

The pressurization system consists of a push-pull syringe containing saline (for biological tissue) or air (for silicone).

During the experiment, the syringe piston is lowered with precision to micro-bar accuracy by means of a controlled actuator. The pressure is increased from 0 to 0.5 bar, in steps of 0.02 bar. At each step reached, a rest time of about 50 s is allowed to avoid viscosity effects. The inflator is a sealed cavity (8 mm of radius) fed by water or air from the pressurization system. A pressure transducer is mounted on it (order no.: HBM 10 bar) and supports the sample between an O-ring and a washer held together by means of 6 screws. There are two cameras to allow the measurement of a field of displacements in 3 dimensions. The model number used for the camera is AlliedVision® Pike F-421B; and for the lens: Fujinon® HF16HA-1B. For the stereo correlation, the software VIC3D® was used. A spray of black paint was sprayed on samples to obtain a speckle.

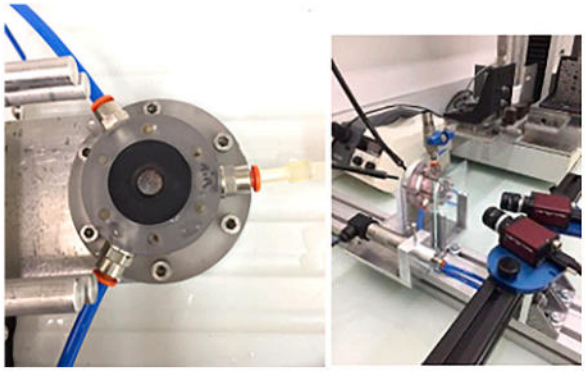

Fig. 2. Inflating device. Front view in the left image. Inflating device with the two cameras in the right image.

For the identification of the material parameters, we have minimized the classical following cost function F:

$$F = \sum_{i}^{N} \left(P^i_{th} - P^i_{exp} \right)^2$$

where

$$P^i_{th} = \frac{h_{init}}{\lambda^i_c \lambda^i_r} \frac{1}{r_i}(\sigma^i_c + \sigma^i_r)$$

is the theoretical pressure calculated by the relation (4) and P^i_{exp} is the experimental pressure, for each loading step i. In the calculation of the theoretical pressure, we took the radius r_i of the sphere fitting the point cloud close to the pole of the deformed surface (see example of sphere fitting in Fig. 4).

For the calculation of the stretch ratios λ^i_c and λ^i_r, we used the relation (2), taken at the pole of the capsule (θ=0 and d0=0). All calculations have been done with the software MATLAB®.

Beside, to validate the identified parameters, a uniaxial tensile test was carried out on silicone in parallel with the bulge tests.

Specimens of length 30 mm, width 6.25 mm and thickness 0.25 mm were used.

The tests were carried out at a displacement speed of 5mm/min.

As before, the displacements of each point of the specimen have been determined using the VIC2D® and VIC3D® software (see Fig. 3).

Three samples from medical silicon sheets of thickness 0.25mm have been tested by each approach (inflation/traction).

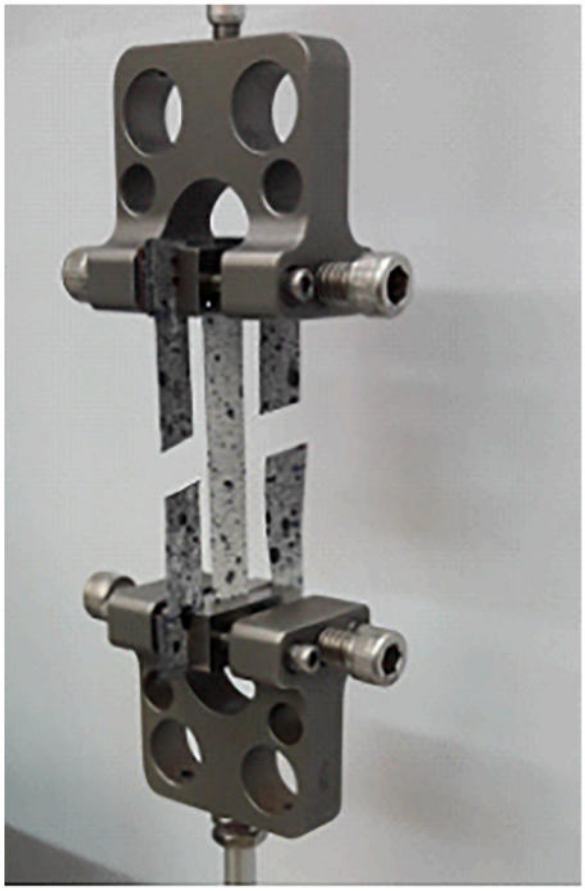

Fig. 3. Tensile device. The silicone sheet is in the center of the clamps.

3.2. Experimental results

3.2.1. Inflation tests

Fig. 4 shows an example of the fitting of the point cloud (yellow points), resulting from the experimental tracking of the capsule surface, by a sphere. This fitting was made by a special MATLAB® function: ellipsoid fit, which calculate the center and the radius of the sphere closest from the point cloud. The results plotted in Fig. 4, were obtained for a maximum pressure of 0.28 bar, during the test corresponding to sample number 2.

The fitting was carried out for each pressure point, giving the radius values of the spheres and allowed the material parameters to be identified (minimizing the cost function F) and the stress-stretch curves to be plotted as shown in Fig. 5.

The experimental stress values plotted in Fig. 5 were calculated with the relation (4), using the values of the stretch ratios λ_c^i, λ_r^i, and the radii r_i from the fitted spheres.

The clusters of crosses, at regular intervals, that we observe on the experimental curve (Fig. 5) represent the relaxation pauses imposed to avoid viscosity effects.

All material parameters, identified from the inflation tests, are gathered in Table 1.

3.2.2. Traction tests

As announced in the previous paragraph, we also carried out uniaxial tensile tests and the identified material parameters are gathered in Table 2.

In this case, there are more differences between the parameter values C10, sometimes from single to double, for an obviously identical material.

There are also differences on the results between the methods of identification of inflation versus traction, but the average values are rather close, and of about 0.29 MPa.

The material coefficients thus identified ensure the positivity of each strain energy for all the elongation values measured during the tests.

4. Numerical approach

Already, at the very beginning of the development of the finite element method, [27,28] proposed an axisymmetric numerical approach for the calculation of stresses and strains in the inflation problem. Since then, many other studies have been conducted with this powerful numerical tool. We can mention the works of [11,26,29–31], which are not limited to elastomers but also deal with metallic and even biological materials.

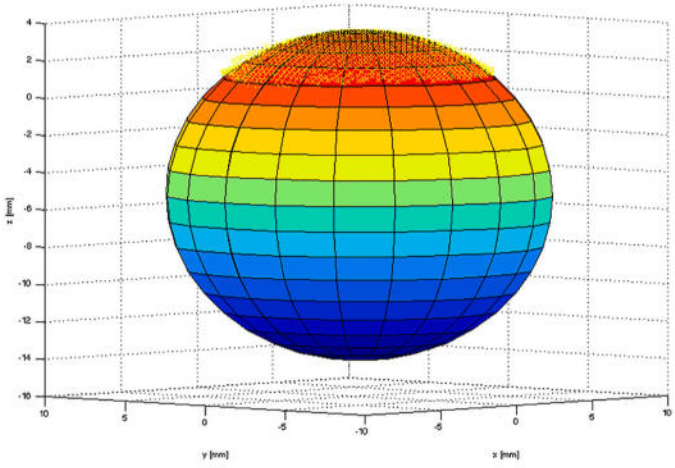

Fig. 4. Fitting of the point cloud (yellow points) by a sphere (Matlab® plot). (For interpretation of the references to colour in this figure legend, the reader is referred to the web version of this article.)

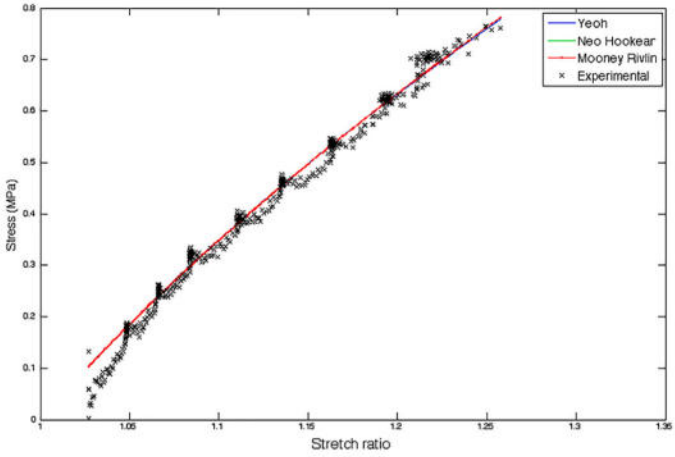

Fig. 5. Stress/Stretch ratio curves and hyperelastic model fitting. Points with crosses come from the experimental measures of sample 2. The curves of the 3 hyperelastic models are confused.

Table 1
Material parameters (in MPa) of the different hyperelastic models identified with the inflating tests.

Models	Parameters	Sample 1	Sample 2	Sample 3	Average
Yeoh	C10	0.227	0.33	0.2	0,25
	C20	0.013	-0.003	1.8e-4	3.39e-03
Mooney-Rivlin	C10	0.228	0.33	0.2	0.25
	C01	1.8e-4	-2.2e-4	-3.7e-5	-2.57e-05
Neo-Hookean	C10	0.228	0.33	0.2	0.25

Note that the values of parameters C10 are very close for each model and the average value is of 0.25 MPa.

Table 2
Material parameters (in MPa) of the different hyperelastic models identified with the tensile tests.

Models	Parameters	Sample 1	Sample 2	Sample 3	Average
Yeoh	C10	0.26	0.42	0.19	0.29
	C20	-0.01	-0.02	0.02	-0.003
Mooney-Rivlin	C10	0.18	0.27	0.29	0.256
	C01	0.10	0.17	-0.12	0.05
Neo-Hookean	C10	0.24	0.41	0.21	0.286

For the numerical validation we also used the finite element method through the software ANSYS®.

4.1. FEM modeling

A circular membrane with a radius of 8mm, blocked on its circumference, was modeled in 3D (surface body). It was subjected to a variable pressure (linear as a function of time), varying from 0 to 0.28 bar. The node displacements of the disk boundary are blocked, but the rotations are free. The problem was treated in quasi-static and large strains. The calculations were done with a two-parameter hyperelastic Yeoh model. We chose the values of C10 and C20 from sample 2 of Table 1. The mesh (Fig. 6) contains quadrangular membrane elements (no rigidity in flexion) with a total of 6,064 nodes.

4.2. FEM results

Fig. 7 shows the vertical displacement isovalues (in meter) of the deformed membrane at the end of loading.

In the software ANSYS®, for hyperelastic models, the deformations

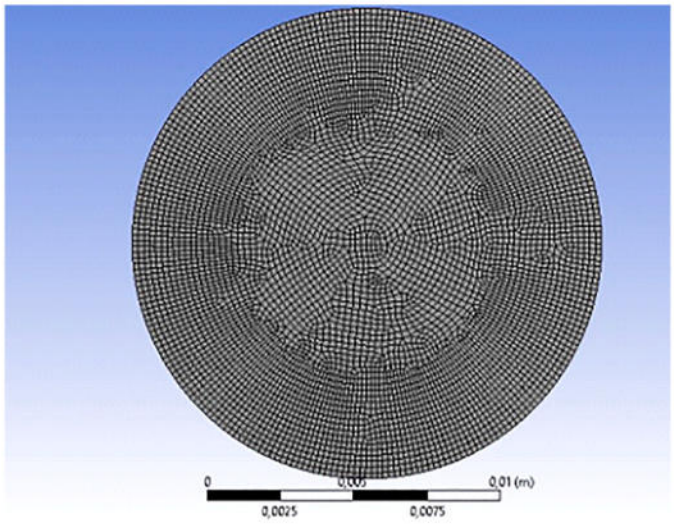

Fig. 6. Mesh of the membrane containing quadrangular membrane elements (no rigidity in flexion) with a total of 6064 nodes.

calculated are those of Green-Lagrange. The principal strains (*Er* and *Ec*) were collected along the x-axis (see Fig. 8) and compared to those calculated by the semi-analytical method (SAM).

The results along this axis are plotted in Fig. 9.

5. Strain comparisons between FEM and SAM

For the SAM, only one of the two strains has been plotted (in green in Fig. 9), as they are assumed to be equal. For their calculation, we used the following relationships:

$$E_c = \frac{1}{2}\left(\lambda_c^2 - 1\right) = E_r = \frac{1}{2}\left(\lambda_r^2 - 1\right)$$

The stretch ratios have been computed using Eq. (2), varying d0 from 0 to $r = 8$ mm, assuming $R = 8.9$ mm (radius of the experimental fitted sphere at the end of the loading) and calculating θ, by solving the non-linear Eq. (3) with a Newton-Raphson algorithm.

Before presenting the deformation results, we performed a verification of the dimensional parameters of the capsule according to the work of Joye et al. [31]. In the paper [31], a correspondence between the two ratios R/r and h/r was established, where h represents the capsule height at the pole. For h=5 mm (calculated experimentally and numerically), we obtained R/r=1.11 and h/r=0.625, which are in agreement with Joye et al.'s results.

The numerical results from the FEM clearly show, in accordance with the literature, a divergence of radial and circumferential strain values the further away from the center of the disk. Concerning SAM results, note that the values for d0=0 and d0=r, are particular because for d0=0 the formula (3) is not defined and for d0=r, it is the formula (2) which is not defined. However, we can still calculate the stretch-ratio values, taking formula (2) in the case where d0=0 and formula (1) in the other case.

The strains calculated by the SAM follow the pattern of the circumferential FEM values and overestimating them. In this example, up to half of the disk, strains calculated by the SAM give a correct approximation of the deformation with respect to radial and circumferential FEM strains. Beyond that, the values (radial and circumferential) differ too much to be approximated by a single value.

6. Discussion and limitations

Our identification approach considers both DIC and the shape of the capsule avoiding uncertainties about the exact position of the top of the membrane, when calculate deflections. The advantage of our method is that it is not necessary to compute average values, at each pressure load. Everything is contained in the approximation of the point cloud by a

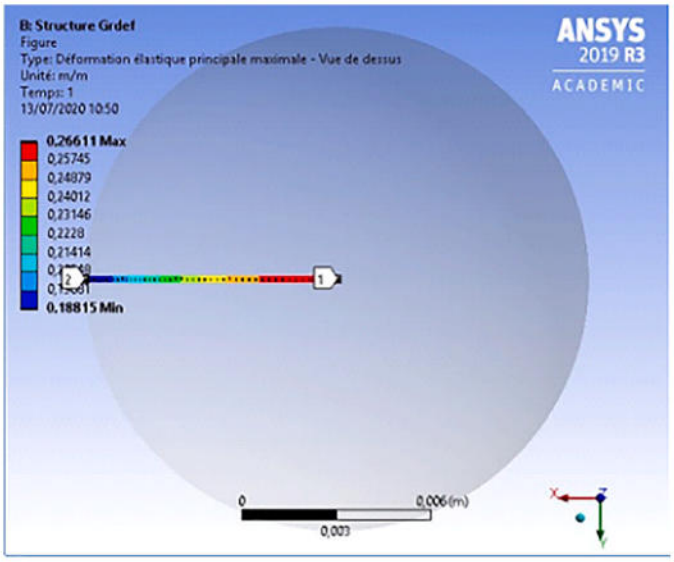

Fig. 8. Isovalues of the Green-Lagrange principal strains (Er and Ec) along the x-axis.

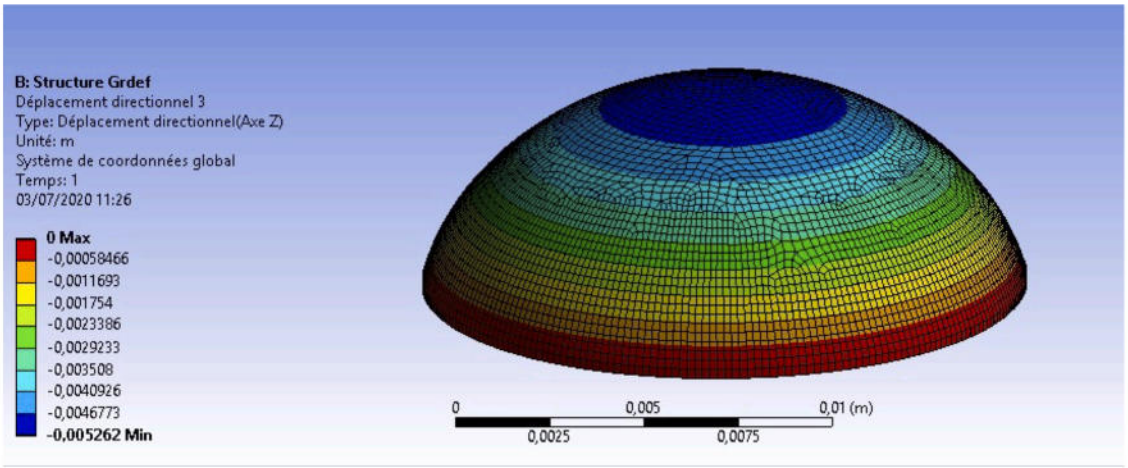

Fig. 7. Vertical displacement isovalues (in meter) of the deformed membrane at the end of loading.

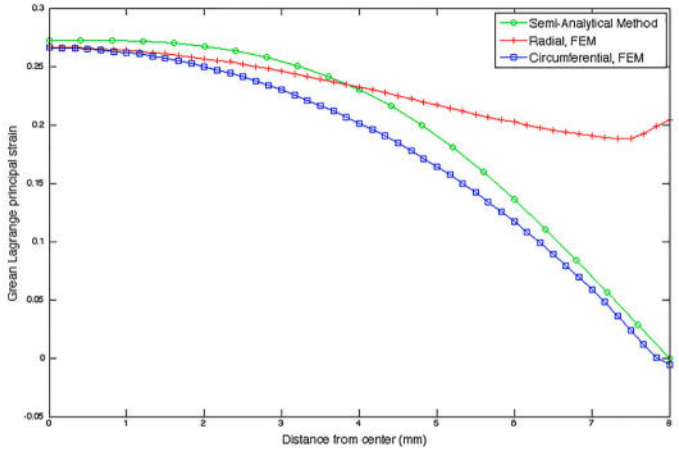

Fig. 9. Comparison of FEM and SAM Green-Lagrange principal strains. SAM results are in green while they are red and blue for the FEM.

sphere.

As this study was performed to test biological tissues, the mechanical bulging loads were performed in a physiological range (stretch-ratios <1.5). Thus, the results obtained show a low nonlinearity of the stress/strain response, which does not allow to differentiate between the different hyperelastic models. This is one of the limitations of the study.

The number of tests (3) remains limited compared to what can be classically found in the literature, but they were relatively reproducible with this type of standard material.

Note that we could have used an axisymmetric 2D model for the numerical simulation, but we decided to use a membrane approximation to be as close as possible to the experimental tests, like work of [26,15].

Discrepancies between the SAM results and FE predictions are mainly due to the approximation chosen for the elongations and because the problem is not equibiaxial.

It should be noted that no tuning has been made to adjust the numerical parameters to best fit the analytical results. These are raw results.

The method (SAM) gives a relatively simple and original semi-analytical solution of the deformation and thus of the stresses during an inflating test but is only valid "close" to the pole. This is another limitation of the study.

7. Conclusion and perspectives

It was developed in this article, a semi-analytical, simple, and original method (SAM) to determine the principal strains during an inflation test of isotropic soft membranes. Its validation was obtained by coupling two complementary approaches.

The first approach was experimental. Inflation and uniaxial tensile tests were set up on medical silicone sheets to identify their hyperelastic constitutive parameters. Then, we injected these mechanical properties into a 3D finite element model of membrane, simulating the inflation test, to compare the strains that had been obtained with those of the SAM.

Numerical results have shown that the strain calculated by the SAM follows the pattern of the circumferential strain obtained by the FEM. Up to a certain distance from the center of the disk (half of the disk for our example), strains calculated by the SAM give a correct approximation of the deformation with respect to radial and circumferential FEM strains.

The methodology implemented in this paper will allow to identify the hyperelastic behavior of biological membrane tissues, weakly anisotropic and to estimate the intensity of deformations close to the pole. This will then allow these deformation values to be compared with the rupture limits, for example those established for cerebral [32,33] or aortic aneurysms [34,35].

Declaration of Competing Interest

The authors declare that they have no known competing financial interests or personal relationships that could have appeared to influence the work reported in this paper.

Data Availability

Data will be made available on request.

References

[1] P. Mott, C. Roland, S. Hassan, Strains in an inflated rubber sheet Rubber, Chem. Technol. 76 (2) (2003) 326–333.
[2] J.E. Adkins, R.S. Rivlin, Large elastic deformations of isotropic materials, IX. The deformation of thin shells, Philos. Trans. R. Soc. Lond. A 244 (1952) 505–531.
[3] L.J. Hart-Smith, J.D.C. Crisp, Large elastic deformations of thin rubber membranes, Int. J. Eng. Sci. 5 (1) (1967) 1–24.
[4] Yang, Feng, On axisymmetrical deformztions of nonlinear membranes, J. Appl. Mech. ASME 37 (1970) 1007–1011.
[5] F.P.K. Hsu, C. Schwab, D. Rigamonti, J.D. Humphrey, Identification of response functions from axisymmetric membrane inflation tests: implications for biomechanics, Int. J. Solids Struct. 31 (24) (1994) 3375–3386.
[6] T. Tsakalakos, The bulge test: a comparison of the theory and experiment for isotropic and anisotropic films, Thin Solid films 75 (3) (1981) 293–305.
[7] K.B.G. Brunon, M. Coret, Characterization of the nonlinear behaviour and the failure of human liver capsule through inflation tests, J. Mech. Behav. Biomed. Mater. 4 (8) (2011) 1572–1581.
[8] T.K. Tonge, L.S. Atlan, L.M. Voo, T.D. Nguyen, Full- field bulge test for planar anisotropic tissues : Part i – experimental methods applied to human skin tissue, Acta Biomater 9 (4) (2013) 5913–5925.
[9] T.K. Tonge, L.S. Atlan, L.M. Voo, T.D. Nguyen, Full-field bulge test for planar anisotropic tissues : Part ii – a thin shell method for determining material parameters and comparison of two distributed fiber modeling approaches, Acta Biomater. 9 (4) (2013) 5926–5942.
[10] S. Avril, Advances in experimental mechanics for biomedical soft tissues and materials strain 5 (52), 371, (2016).
[11] L. Meunier, G. Chagnon, D. Favier, L. Orgeas, P. Vacher, Mechanical experimental characterisation and numerical modelling of an unfilled silicone rubber, Polym. Test. 27 (2008) 765–777.
[12] M. Sasso, G. Palmieri, G. Chiappini, D. Amodio, Characterization of hyperelastic rubber-like materials by biaxial and uniaxial stretching tests based on optical methods, Polym. Test. 27 (2008) 995–1004.
[13] Y. Li, J.A. Nemes, A.A. Derdouri, Membrane inflation of polymeric materials: experiments and finite element simulations, Polym. Eng. Sci. 41 (8) (2001) 1399–1412.
[14] L. Thangawng, R.S. Ruoff, M.A. Swartz, M.R. Glucksberg, An ultra-thin PDMS membrane as a bio/micro-nano interface: fabrication and characterization, Biomed. Microdevices 9 (4) (2007) 587–595.
[15] M.R. Mansouri, H. Darijani, M. Baghani, On the correlation of FEM and experiments for hyperelastic elastomers, Exp. Mech. 57 (2017) 195–206.
[16] N. Reuge, F.M. Schmidt, Y.Le Maoult, M. Rachik, F. Abbé, Elastomer biaxial characterization using bubble inflation technique. I: experimental investigations, Polym. Eng. Sci. 41 (3) (2001) 522–531.
[17] L.R.G. Treloar, Strains in an inflated rubber sheet and the mechanism of bursting, Trans. of the Institution of Rubber Industry 19 (1944) 201–212.
[18] R. Johannknecht, G. Clauss, S. Jerrams, Determination of non-linear, large, equal biaxial stresses and strains in thin elastomeric sheets by bubble inflation, Proc. Inst. Mech. Eng. Part L J. Mater. Des. Appl. 216 (2002).
[19] M. Mooney, J. Appl. Phys. 11 (1940) 582.
[20] M. Mooney, J. Appl. Phys. 19 (1948) 434.
[21] R.S. Rivlin, Philos. Trans. R. Soc. Lond. Ser. A 240 (1948) 459.
[22] R.S. Rivlin, Philos. Trans. R. Soc. Lond. Ser. A 241 (1948) 379.
[23] O.H. Yeoh, (O.H.), Some forms of the strain energy function for rubber, Rubber Chem. Technol. 66 (5) (1993) 754–771.
[24] L.R.G. Treloar, The elasticity of a network of long chain molecules (I and II), Trans. Faraday Soc. 39 (1943) 36–64, 241–246.
[25] S. Wineman, D. Wilson, J.W. Melvin, Material identification of soft tissue using membrane inflation, J. Biomech. 12 (1979) 841–850.
[26] G. Machado, D. Favier, G. Chagnon, Membrane curvatures and stress-strain full fields of axisymmetric bulge tests from 3D-DIC measurements. Theory and validation on virtual and experimental results, Exp. Mech. 52 (7) (2012) 865–880.
[27] S.C. Tang, Large strain analysis of an inflating membrane, Comput. Struct. 15 (1) (1982) 71–78.
[28] Fried, Finite element computation of large rubber membrane deformations, Int. J. Numer. Methods Eng. 18 (5) (1982) 653–660.
[29] J.C. Selby, M.A. Shannon, Inflation of a circular elastomeric membrane into a horizontally semi-infinite liquid reservoir of finite vertical depth: quasi-static deformation model, Int. J. Eng. Sci. 47 (5-6) (2009) 700–717.

[30] K. Balakhovsky, K.Y. Volokh, Inflation and rupture of rubber membrane, Int. J. Fract. 177 (2) (2012) 179–190.
[31] D.D. Joye, G.W. Poehlein, C.D. et Denson, A bubble inflation technique for the measurement of viscoelastic properties in equal biaxial extensional flow, Trans. Soc. Rheol. 16 (3) (1972) 421–445.
[32] H. Brunel, D. Ambard, H. Dufour, P.H. Roche, V. Costalat, F. Jourdan, Rupture limit evaluation of human cerebral aneurysms wall: experimental study, J. Biomech. 77 (2018) 76–82.
[33] D. Parshin, A. Lipovka, A. Dubovoy, M. Vasilyeva, E. Kuznetsova, D. Sergeevichev, Different stages of the evolution of cerebral aneurysms: joint analysis of mechanical test data and histological analysis of aneurysm tissue, EPJ Web Conf. 221 (2019) 01028. EDP Sciences.
[34] D.A. Vorp, B.J. Schiro, M.P. Ehrlich, T.S. Juvonen, M.A Ergin, B.P Griffith, Effect of aneurysm on the tensile strength and biomechanical behavior of the ascending thoracic aorta, Ann. Thorac. Surg. 75 (4) (2003) 1210–1214.
[35] O.T Duprey, M. Vola, J.P. Favre, S. Avril, Biaxial rupture properties of ascending thoracic aortic aneurysms, Acta Biomater. 42 (2016) 273–285.